Rare Metal Materials and Engineering
Volume 51, Issue 12, December 2022
Available online at www.rmme.ac.cn

Science Press

Cite this article as: Qi Boyi, Liu Chengze, Yang Qinghao, et al. Stress Corrosion Cracking Behavior of Commercial Zr702 in Boiling Nitric Acid Solutions for Spent Nuclear Fuel Reprocessing[J]. Rare Metal Materials and Engineering, 2022, 51(12): 4483-4487.

ARTICLE

Stress Corrosion Cracking Behavior of Commercial Zr702 in Boiling Nitric Acid Solutions for Spent Nuclear Fuel Reprocessing

Qi Boyi[1,2], Liu Chengze[2], Yang Qinghao[1], Xu Jianping[2,3], Liu Lu[2], Qiu Longshi[2], Zhang Yusheng[2]

[1] School of Materials Science and Engineering, Xi'an University of Science and Technology, Xi'an 710054, China; [2] Xi'an Rare Metal Materials Institute Co., Ltd, Xi'an 710016, China; [3] State Key Laboratory for Mechanical Behavior of Materials, Xi'an Jiaotong University, Xi'an 710049, China

Abstract: The stress corrosion cracking (SCC) and its susceptibility (I_{SCC}) of commercial Zr702 applied for spent nuclear fuel reprocessing industry was investigated in boiling nitric acid. Stress-strain curves of Zr702 in boiling nitric acid with strain rate of 10^{-5} s^{-1} were obtained using independent designed slow strain rate tension (SSRT) system. Microscopic characterizations as well as numerical analysis were carried out to quantify the SCC behavior of Zr702. Results reveal that the I_{SCC} of Zr702 obviously increases from 5% to 26.67% with the increase in HNO_3 concentration. The sharp decline in the mechanical properties of commercial Zr702 in boiling HNO_3 solutions is attributed to cleavage fracture on surfaces of specimen, and the depth of the cleavage cracks increases with the growing HNO_3 concentration. Finally, a model and an equation to predict the SCC behavior of commercial Zr702 in boiling HNO_3 solutions was proposed. The quantitative relationship among HNO_3 concentration, I_{SCC}, fracture stress (σ_{SCC}) and cleavage crack depth (d_{cc}) can be described and predicted using a high-order regression equation.

Key words: reprocessing; Zr702; stress corrosion cracking; SSRT

Nuclear power began out of military necessity, but since its inception, this unprecedented power has shown great potential in electricity generation[1-5]. At present, nuclear power plants meet over 13% of the world's electricity demand[6]. For example, nuclear power accounts for 72.28% of the energy compo-sition of France[7]. Nuclear reprocessing plays an important role in the nuclear fuel cycle, and reprocessing of spent nuclear fuels (SNF) has been carried out usually in concentrated boiling nitric acid solutions[8-10]. Therefore, structural materials used in nuclear fuel reprocessing plants require superior corrosion resistance and reliability.

In India, stainless steels are now indispensable constructional materials for dealing with HNO_3, since they have good corrosion resistance against nitric acid solutions as well as appropriate practical properties such as working and welding properties. However, there are some drawbacks, i.e. they are susceptible to general and intergranular corrosion in highly oxidizing nitric acid media which contains oxidizing reagents such as Cr^{6+} and Ce^{4+} with high oxidation-reduction potentials[11].

Based on security considerations, damage related properties are important to these materials working in complex environment for long time. Zirconium and its alloys are extensively used in the cores of water-cooled nuclear reactors mainly because of their low thermal neutron absorption cross-section, reasonable mechanical and excellent corrosion resistance under operating conditions. Compared with other alloys, Zr and its series alloys such as Zr702 have a relatively good corrosion resistance[12-14].

It has been demonstrated that Zr exhibits excellent resis-

Received date: February 21, 2022
Foundation item: Natural Science Foundation of Shaanxi Province (2020JC-50, 2020JQ-924, 2020GY-268); Xi'an Science and Technology Plan Project (2020YZ0028); RMMI Research Project (Y1905S)
Corresponding author: Yang Qinghao, Ph. D., Professor, School of Materials Science and Engineering, Xi'an University of Science and Technology, Xi'an 710054, P. R. China, Tel: 0086-29-85583114, E-mail: yangxjtu@hotmail.com

tance to general corrosion in HNO_3. However, past studies have shown that Zr is susceptible to stress corrosion cracking (SCC) under specific conditions in boiling HNO_3 solutions[15]. Kajimura[11] evaluated SCC susceptibility using slow strain rate tests (SSRT) in a boiling nitric acid solution, and suggested that the corrosion potential for SCC has effects on the susceptibility of zirconium to SCC in a boiling nitric acid solution.

Yau[16] investigated SCC for commercially pure Zr, Zr-l.5% Sn alloy and Zr-2.5%Nb alloy in HNO_3 by the U-bend and C-ring tests, and reported that although all of them have high SCC resistance in 70% HNO_3 up to the boiling point, they become susceptible to SCC in HNO_3 above 80%. Recently, it has been reported that besides alloying, grain size can also affect the corrosion behavior of metals[17].

However, most early investigations of the corrosion behavior of zirconium and its alloys in a boiling nitric acid solution focus on similar concentrations. These reports lack the consensus in the reported data about the effect of nitric acid concentration on the corrosion resistance and the proposed mechanisms are often conflicting or unclear, which introduces considerable uncertainty into the subsequent analysis.

To obtain an optimal processing method for improving the SCC resistance of zirconium alloys, it is necessary to understand the possible cracking modes and to establish their relationship at different concentrations of nitric acid. This study presented microscopic evaluation of crack initiation and propagation characteristics of Zr702 at different concentrations of boiling nitric acid, aiming to obtain available data to better investigate the behavior of Zr702. For this purpose, stress-strain curves and initial microstructure, etc as factors affecting the crack initiation were analyzed.

1 Experiment

The material used in this study was commercial Zr702, and its measured chemical composition is shown in Table 1. Zr702 plate with 28 mm in thickness was manufactured by vacuum arc melting, forging, and hot rolling, followed by annealing at 800 °C for 1 h. Samples with three cross sections were obtained by an electrical discharge machine along the normal direction (ND), rolling direction (RD) and transverse direction (TD) planes. Sectional surfaces were mechanically ground step by step with abrasive paper, followed by mechanical polishing using a colloidal silica suspension. Etching with an acid mixture of alcohol: HF=9: 1 in volume ratio was carried out for metallographic analysis, which is shown in Fig. 1a. To perform SCC analysis of Zr702 in boiling HNO_3 solutions, customized testing system as well as SSRT specimen were designed correspondingly.

As shown in Fig. 1b, the testing system is mainly composed of heater, test cell and condenser. During the experiments, the HNO_3 in the test cell was boiled by the heater, and the solution

Table 1 Chemical composition of commercial Zr702 (wt%)

H	C	N	O	Fe+Cr	Hf	Zr
0.0010	0.007	0.009	0.079	0.0321	2.14	Bal.

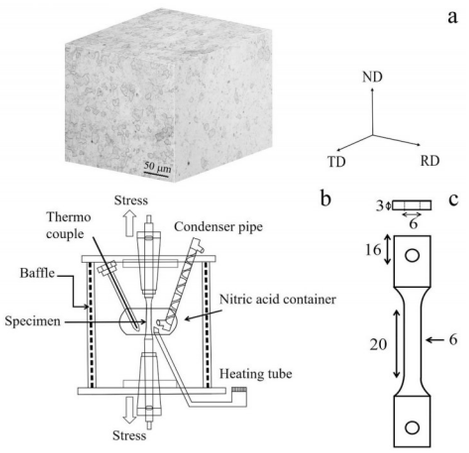

Fig.1 Optical microstructure of Zr702 plate viewed along three directions (a), schematic diagram of SSRT testing system (b), and specimen geometry and dimensions for SSRT tests (c)

condensed in the glass condenser was collected into the glass collector located under the condenser in the test cell. The strain rate was controlled by a contact extensometer to remove the effect of equipment stiffness. The extensometer had enough length, which created a relatively close strain rate even in the elastic zone. The SSRT tests were carried out in different HNO_3 concentrations (0, 4, 8 and 14.4, mol/L). Among them, the 0 mol/L HNO_3 test was carried out in pure boiling water.

SSRT specimens, whose geometry and dimensions are shown in Fig. 1c, were extracted from the Zr702 plate along RD. Their gauge parts (20 mm in length, 6 mm in width and 3 mm in thickness) were all mechanically ground by abrasive paper, followed by ultrasonic cleaning in alcohol. Specimens were deformed to failure at strain rate of 1×10^{-5} s^{-1} during SSRT tests, and then kept under open-circuit electro-chemical potential conditions. The effect of HNO_3 concen-tration on SCC at boiling temperature was evaluated by stress-strain curve. Both fracture and lateral surfaces of the specimens after SSRT were characterized by OPTON: HS-OP-810 scanning electron microscope (SEM).

2 Results and Discussion

Fig. 2a shows the engineering stress-strain curves of Zr702 with strain rate of 1×10^{-5} s^{-1} in boiling water as well as HNO_3 solutions. The results show that the specimens under all conditions have uniform plastic deformation zone, and the specimens exhibit relatively long softening behavior after reaching the ultimate tensile strength (UTS).

The elongation of the tested specimens changes with the HNO_3 concentration, all in the range of 35% to 45%. This result confirms that the plasticity of the commercial Zr702 is affected by the concentration of HNO_3 during SSRT.

The final fracture surfaces of commercial Zr702 specimens after SSRT are shown in Fig. 2c~2f. It can be observed that all the specimens show ductile fracture characteristics. In order to evaluate the effect of HNO_3 concentration on plastic fracture, the fracture dimple size of all the tested specimens were

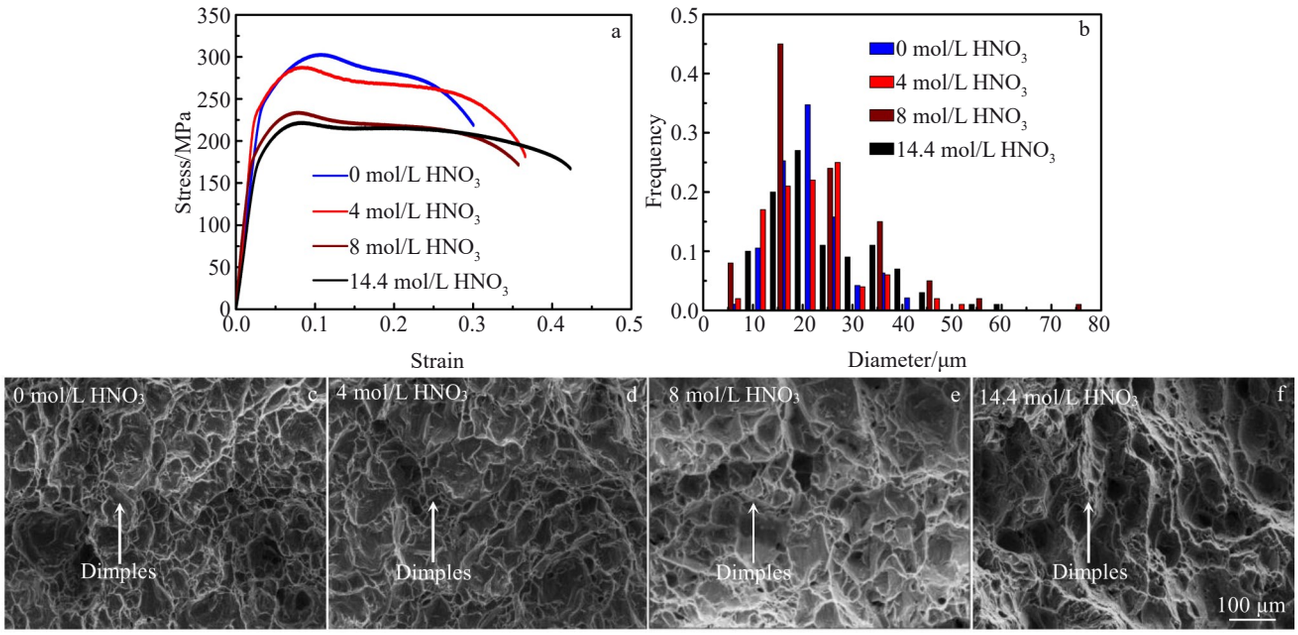

Fig.2 Engineering stress-strain curves of Zr702 in different HNO_3 solutions (a), dimple size of the fractography (center region) of specimens (b), and SEM images of fractured commercial Zr702 specimens after SSRT tests in boiling HNO_3 solutions with different concentrations (c~f)

measured. By fitting with Gaussian curve, it is found that the average dimple size of the specimens is 16.04~21.55 μm.

The specimen tested in the lowest-concentration HNO_3 presents the highest fracture strength (300 MPa), whereas the lowest fracture strength (220 MPa) is obtained at the highest concentration of HNO_3. Thus, it is clear that commercial Zr702 exhibit SCC sensitivity in boiling HNO_3 solutions.

The SCC susceptibility index (I_{SCC}) determined by the loss of fracture stress measured in a solution is given by following equation[18]

$$I_{SCC}(\sigma)=(1-\sigma_{SCC}/\sigma_0)\times100\% \quad (1)$$

where $I_{SCC}(\sigma)$ is the stress corrosion susceptibility (%), σ_{SCC} is the fracture stress in corrosive medium (MPa) and σ_0 is the fracture stress in inert media (MPa).

The calculated I_{SCC} of the commercial Zr702 in boiling HNO_3 solutions is summarized in Table 2. It can be clearly seen that with increasing the HNO_3 concentration, I_{SCC} is significantly increased from 5% to 26.67%.

In a recent study, Chiaki Kato[19] reported that SCC behavior of Zr alloy was studied using slow strain rate testing (SSRT) technique in HNO_3 (8 mol/L), and they found that no significant decrease in the ultimate tensile strength is observed for specimens tested in HNO_3 compared to specimens tested in air. The experimental comparison shows that different composition of Zr alloy leads to SCC.

Table 2 SCC sensitivity of commercial Zr702 measured by SSRT in boiling nitric acid with different concentrations

HNO_3 concentration/mol·L^{-1}	Strain rate/s^{-1}	σ_{SCC}	$I_{SCC}(\sigma)$/%
0	1×10^{-5}	300	0
4		285	5
8		230	23.33
14.4		220	26.67

To understand the SCC mechanism of commercial Zr702 in boiling HNO_3 solutions, the cracking initiation behavior was further analyzed by SEM. As shown in Fig. $3a_1$~$3d_1$, high-magnification micrograph of the crack initiation region of the specimens tested in water and HNO_3 solutions shows distinct characteristics. The crack initiation region of the specimens tested in water contains dimples, whereas that in HNO_3 solutions shows typical cleavage facets. According to Fig.3, it can be concluded that the fracture surfaces of commercial Zr702 tested in HNO_3 contains two distinct regions, which show cleavage feature at cracking initiation region and ductile feature in the rest center region, correspondingly. To evaluate the effect of HNO_3 concentration on the cracking initiation behavior, d_{CC} was introduced, which represents the depth of the cleavage crack. This value is measured to be 0, 169.19, 191.67 and 206.66 μm for specimens tested in 0, 4, 8 and 14.4 mol/L HNO_3 solutions, respectively.

The lateral surfaces of the Zr702 specimens are presented in Fig. $3a_2$~$3d_2$. Cleavage cracks, which are distributed perpendicular to the tensile direction, are observed in specimens tested in HNO_3 solutions without exceptions, while it is not detected in specimens tested in water. In addition, as the concentration of HNO_3 increases, the depth of these cleavage cracks on the lateral surfaces increases, which will increase the SCC susceptibility of commercial Zr702[20]. It also agrees with the calculated SCC susceptibility index.

The corrosion resistance of zirconium is excellent in boiling nitric acid[21], as shown in Fig. 2a, while the performance of

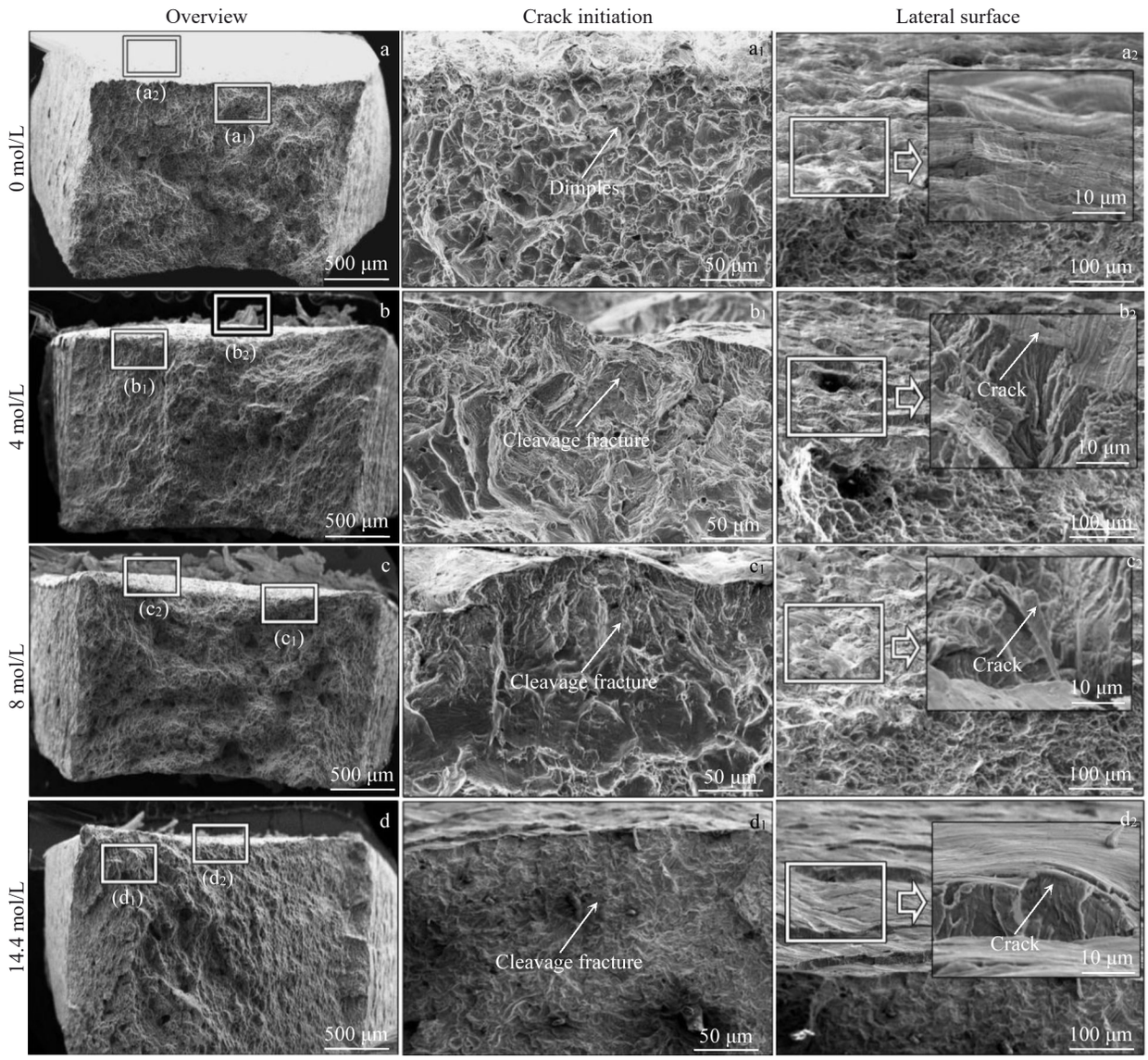

Fig.3 SEM images of fractured commercial Zr702 specimens after SSRT tests in boiling HNO_3 solutions with different concentrations

Zr702 is reduced under the combined effects of strain and corrosion. In order to further understand the effect of HNO_3 concentration on SCC behavior of commercial Zr702, numerical analysis was carried out to quantify the relationship among I_{SCC}, σ_{SCC} and d_{cc}. Equations among these parameters were finally proposed, and the detailed process for the derivation of the formula was described in the supplementary material.

$$I_{SCC}=0.5163x^2-15.96x+327.5 \quad (2)$$

$$\sigma_{SCC}=-0.0914x^2+3.3585x-1.8496 \quad (3)$$

$$d_{cc}=0.3104x^3-8.3096x^2+0.5694x \quad (4)$$

where x is HNO_3 concentration. It can be used to determine the key optimizing operating parameters of Zr702 stress corrosion sensitivity in HNO_3. Although the applicability of the formula is limited due to the number of experiments, it has certain guiding significances for future research on the stress corrosion behavior of different metals HNO_3.

Based on the above equations, the function fitting curves are obtained and shown in Fig. 4a. The output value is approximately linear with the expected value, showing a high degree of correlation. Comparison of the SCC susceptibility, facture stress and cleavage crack depth of specimens tested in different HNO_3 solutions is shown in Fig.4a.

Moreover, according to the measured results, the depth of cleavage cracks is deepened with increasing the HNO_3 concentration, which leads to decrease in cross-sectional areas and finally reduces the engineering strength. Fig. 4b and 4c represent schematic diagrams of the samples tested in water and environment, respectively. Blue and red lines refer to dimples and cleavage cracks. During SSRT tests in boiling water, the fracture mode of commercial Zr702 is typically ductile fracture, evidenced by high-density dimples in the fracture surface. However, during SSRT in boiling HNO_3 solutions, cleavage cracks are firstly initiated on outer surfaces of specimen, which is the oxide layer. In the subsequent straining process, ductile fracture takes place and leads to final fracture. The drop-down of fracture stress is attributed to these cleavage cracks resulted from the failure of oxide layers.

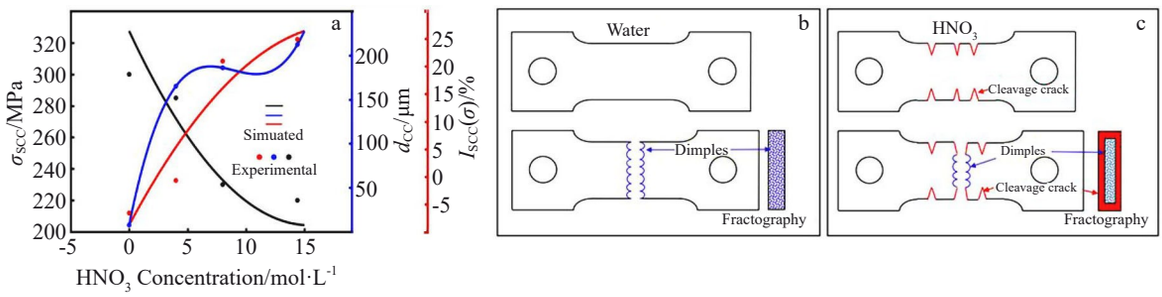

Fig.4 High-order fitting curves of SCC susceptibility (I_{SCC}), facture stress (σ_{SCC}) and cleavage crack depth (d_{cc}) (a), schematic diagrams of the fracture mechanism of commercial Zr702 during SSRT in boiling water (b) and HNO_3 solutions (c)

3 Conclusions

1) HNO_3 can affect the fracture mode of commercial Zr702 during slow strain rate tension (SSRT) tests. The specimens tested in boiling water show typical ductile fracture feature, while in boiling HNO_3 solutions, the fracture mode is the mixture of cleavage cracking initiation and ductile fracture.

2) With increasing the HNO_3 concentration, the depth of cleavage cracks (d_{cc}) increases from 169.19 to 206.66 μm, which explains the drop-down of fracture stress (σ_{SCC}) and the increment of stress corrosion susceptibility (I_{SCC}).

3) The quantitative relationship among HNO_3 concentration, I_{SCC}, σ_{SCC} and d_{cc} can be described and predicted using a high-order regression equation.

References

1 Shahi E, Alavipoor F S, Karimi S. *Renewable and Sustainable Energy Reviews*[J], 2018, 83: 33
2 Jenkins J D, Zhou Z, Ponciroli R *et al. Applied Energy*[J], 2018, 222: 872
3 Wang Z Y, Pedroni N, Zentner Irmela *et al. Eng Struct*[J], 2018, 162: 213
4 Cany C, Mansilla C, Mathonniere G *et al. Energy*[J], 2018, 151: 289
5 Xiao X J, Jiang K J. *Advances in Climate Change Research*[J], 2018, 9(2): 6
6 Cabrera C, Estanislau F, Pereira C *et al. Energy Strategy Reviews*[J], 2020, 30: 100 513
7 Cox B. *Journal of Nuclear Materials*[J], 2005, 336(2-3): 331
8 Sudhakar, Rao G *et al. Journal of Nuclear Materials: Materials Aspects of Fission and Fusion*[J], 2013, 441(1-3): 455
9 Ishijima Y, Kato C, Motooka T *et al. Mater Trans*[J], 2013, 54: 1001
10 Yamamoto M, Kato C, Ishijima Y *et al. ECS Transactions*[J], 2009, 16(52): 101
11 Kajimura H, Nagano H, Miura. *US Patent*[P], 1987
12 Bishop C R. *Corrosion Engineering* [J], 1963, 19(9): 308
13 Wande C F. *Nuclear Physics*[J], 1958, 9(4): 693
14 Zou D B Luan D X. *Rare Metal Materials and Engineering*[J], 2014, 43(8): 1897
15 Nagano H, Kajimura H. *Corrosion Science*[J], 1996: 782
16 Yau T L, Webster R T. *Corrosion*[J], 1983, 39(6): 218
17 Bagha P S, Khakbiz M, Sheibani S *et al. J Alloys Compd*[J], 2018, 67(7): 955
18 Zhu Wuyang. *Hydrogen Embrittlement and Stress Corrosion Cracking*[M]. Beijing: Science Press, 2013: 367 (in Chinese)
19 Chiaki Kato. *Thesis for Doctorate*[D]. Tokyo : Tokyo Institute of Technology, 2002
20 Jayaraj J, Krishnaveni P, Krishna D *et al. Journal of Nuclear Materials*[J], 2016, 473: 157
21 Creus J, Lagarde M, Nia N S *et al. Rare Metal Materials & Engineering*[J], 2015, 44(5): 1169

用于乏核燃料后处理的商用 Zr702 在沸腾硝酸溶液中的应力腐蚀开裂行为

齐博毅[1,2]，刘承泽[2]，杨庆浩[1]，徐建平[2,3]，刘　璐[2]，邱龙时[2]，张于胜[2]

(1. 西安科技大学 材料科学与工程学院，陕西 西安 710054)

(2. 西安稀有金属材料研究院有限公司，陕西 西安 710016)

(3. 西安交通大学 金属材料强度国家重点实验室，陕西 西安 710049)

摘　要：研究了商用Zr702在沸腾硝酸中应用于乏核燃料后处理工业的应力腐蚀开裂（SCC）行为和应力腐蚀敏感性（I_{SCC}）。使用独立设计的慢应变率拉伸（SSRT）系统在沸腾的硝酸中获得应变率为10^{-5} s^{-1}的Zr702的应力-应变曲线。进行微观表征以及数值分析以量化Zr702的SCC行为。结果表明，随着HNO_3浓度的增加，Zr702的I_{SCC}由5%明显增加到26.67%。商用Zr702在沸腾HNO_3溶液中力学性能的急剧下降归因于试样表面的解理断裂，并且解理裂纹的深度随着HNO_3浓度的增加而增加。最后，提出了预测商业Zr702在沸腾HNO_3溶液中SCC行为的模型和方程。HNO_3浓度、I_{SCC}、断裂应力（σ_{SCC}）和解理裂纹深度（d_{cc}）之间的定量关系可以使用高阶回归方程来描述和预测。

关键词：再加工；Zr702；应力腐蚀开裂；慢应变速率拉伸

作者简介：齐博毅，男，1997年生，硕士，西安科技大学材料科学与工程学院，陕西 西安710054，电话：029-84837566，E-mail：291614912@qq.com